ornl

OAK
RIDGE
NATIONAL
LABORATORY

UNION
CARBIDE

ORNL-5605

OAK RIDGE NATIONAL LABORATORY LIBRARIES
3 4456 0571637 5

Materials Heat-to-Heat Variability Study: Part II—Analysis of the Effect on the Conservatism of Current Inelastic High-Temperature Structural Design Procedures

W. K. Sartory W. J. McAfee

OAK RIDGE NATIONAL LABORATORY
CENTRAL RESEARCH LIBRARY
CIRCULATION SECTION
4500N ROOM 175
LIBRARY LOAN COPY
DO NOT TRANSFER TO ANOTHER PERSON
If you wish someone else to see this report, send in name with report and the library will arrange a loan.
UCN-7969 3 9-77

This document does not contain UCNI, ECI, or other unclassified sensitive information and has been approved for release to the public by:

David R. Hamrin 11/10/2010

David R. Hamrin, ORNL Classification Officer Date

[redacted]

OPERATED BY
UNION CARBIDE CORPORATION
FOR THE UNITED STATES
DEPARTMENT OF ENERGY

Printed in the United States of America. Available from
the Department of Energy
Technical Information Center
P.O. Box 62, Oak Ridge, Tennessee 37830
Printed Copy A03 ; Microfiche A01

This report was prepared as an account of work sponsored by an agency of the United States Government. Neither the United States nor any agency thereof, nor any of their employees, makes any warranty, expressed or implied, or assumes any legal liability or responsibility for any third party's use or the results of such use of any information, apparatus, product or process disclosed in this report, or represents that its use by such third party would not infringe privately owned rights.

ORNL-5605
Dist. Category UC-79,
-79h, -79k

Contract No. W-7405-eng-26

Engineering Technology Division

MATERIALS HEAT-TO-HEAT VARIABILITY STUDY: PART II—ANALYSIS OF THE EFFECT ON THE CONSERVATISM OF CURRENT INELASTIC HIGH-TEMPERATURE STRUCTURAL DESIGN PROCEDURES

W. K. Sartory W. J. McAfee

Date Published - December 1979

Prepared by the
OAK RIDGE NATIONAL LABORATORY
Oak Ridge, Tennessee 37830
operated by
UNION CARBIDE CORPORATION
for the
DEPARTMENT OF ENERGY

CONTENTS

	Page
ABSTRACT	1
1. INTRODUCTION	1
2. BASIC PROBLEM DESCRIPTION	3
3. MATERIAL PROPERTIES	5
4. STRUCTURAL ANALYSIS AND DAMAGE EVALUATION	11
4.1 Finite-Element Procedure	11
4.2 Thermal Analysis Procedure	12
4.3 Constitutive Equations	12
4.4 Damage Evaluation	14
5. SENSITIVITY STUDY, DESIGN ANALYSIS, AND THEIR RESULTS	15
5.1 Selection of Quantities to Be Tested for Conservatism	15
5.2 Selection of Analyses Points and Details of Interpolation Procedure	16
5.3 Results of Sensitivity Study	17
5.4 Results of Design Analysis	19
6. ANALYSIS OF CONSERVATISM AND ASSOCIATED RESULTS	24
6.1 Technique Used to Determine Conservatism	24
6.2 Results of Determination of Conservatism	24
6.3 Effect of Possible Added Safety Factors on Percentage of Nonconservatism	25
7. DISCUSSION OF RESULTS	29
8. SUGGESTIONS FOR FUTURE WORK	33
9. SUMMARY AND CONCLUSIONS	34
ACKNOWLEDGMENTS	35
REFERENCES	36

MATERIALS HEAT-TO-HEAT VARIABILITY STUDY: PART II—ANALYSIS OF THE EFFECT ON THE CONSERVATISM OF CURRENT INELASTIC HIGH-TEMPERATURE STRUCTURAL DESIGN PROCEDURES*

W. K. Sartory W. J. McAfee

ABSTRACT

A sensitivity study involving 16 inelastic structural analyses and creep-fatigue damage evaluations was performed to establish the effect of heat-to-heat variability of the creep rate, yield strength, and creep rupture strength on the ratchetting strain, creep and fatigue damage, and cyclic life of a type 304 stainless steel pipe subject to ratchetting loading conditions. The material property data used in the sensitivity study were taken from a statistical evaluation of 20 heats. A design analysis was then performed for the same structure using material properties taken from the *Nuclear Systems Materials Handbook* and The American Society of Mechanical Engineers Code Case N-47 and incorporating the currently recommended design margins or safety factors. By comparing the results of the sensitivity study to the design analysis, the heat-to-heat variability was found to cause the design margins to be overrun for about 1% of all heats with respect to creep damage and the associated cyclic life. For fatigue damage, the percentage of heats for which the design margins were overrun was too small to detect. For ratchetting strain, the design margins are not known. When the assumption was made that there are no design margins for ratchetting strain, the design analysis was found to be nonconservative for a majority of the heats.

Keywords: design conservatism, property variability, Code Case N-47, type 304 stainless steel, ratchetting, creep-fatigue damage, high-temperature structural design, inelastic analysis.

1. INTRODUCTION

One of the facets of the Oak Ridge National Laboratory High-Temperature Structural Design Program is the development of inelastic design analysis methods, criteria, and rules to preclude structural failures. To aid in that development, this report presents the results of an assessment of the conservatism of the present procedures specifically with regard to their ability to compensate for material variability.

Nuclear systems components are sometimes designed by inelastic structural analysis. Even when elastic design rules are used, the conservatism of the elastic rules is often verified by comparison with inelastic analysis results,[1-4] so the conservatism of the inelastic design procedures is still of interest. Performance of an inelastic structural analysis requires that a variety of material properties be specified, for example, the yield stress and creep rate.

Heats of material that are nominally the same (e.g., all type 304 stainless steel) show considerable heat-to-heat variability in their properties. However, the designer usually will not know the properties of the specific heat to be used in fabricating the component that he is designing and, therefore, will necessarily perform the design analysis using material properties taken from the *Nuclear Systems Materials Handbook* (NSMH),[5] or The American Society of Mechanical Engineers Code Case N-47

*Work performed under DOE/RRT 189a OHO48, High-Temperature Structural Design.

(CCN47),[6] or similar sources of the general properties of type 304 stainless steel. Such an analysis will be referred to in this report as a design analysis. The design will be modified, if necessary, until it satisfies the required criteria (e.g., on the cumulative damage and ratchetting strain) based on the design analysis.

When the component is actually fabricated, however, it will be made of a heat with properties somewhat different from the properties used in the design analysis, so the damage and ratchetting strain will also be different. At some stage, sufficient conservatism must be incorporated into the design procedure so that, whenever the design analysis satisfies the required criteria, the component will also satisfy acceptable criteria, regardless of which heat is used in its fabrication. This report determines the effect of heat-to-heat variability of the material properties of type 304 stainless steel on the calculated ratchetting strain, creep and fatigue damage, and cyclic life. A design analysis is also carried out, and its conservatism is evaluated by comparison with the heat-to-heat variability study.

An earlier sensitivity study of the effect of variability in yield strength and creep rate on the ratchetting strain and damage was reported by Corum and Sartory.[7] This study differs because it is more extensive, is based on a more thorough examination of material variability, and is applied to a direct statistical assessment of the conservatism of the design margins of CCN47.

In a related work, the advantages of using consistent creep and rupture data are discussed by Schultz.[8]

2. BASIC PROBLEM DESCRIPTION

The analyses presented in this report are all based on a single problem—a long pipe of type 304 stainless steel subjected to a ratchetting load condition. The pipe geometry and loads are presented in Table 2.1.

The load histogram is shown in Fig. 2.1. It consists of a coolant thermal downshock from 593 to 427° C (1100 to 800° F) in 10 s. The heat transfer coefficient from the coolant to the inner surface of the

Table 2.1. Pipe geometry and load conditions for basic ratchetting problem

Parameter	Value
Outer pipe radius, mm (in.)	107.19 (4.22)
Inner pipe radius, mm (in.)	97.66 (3.845)
Pipe wall, mm (in.)	9.53 (0.375)
Downshock rate, °C/s (°F/sec)	16.67 (30)
Internal pressure, MPa (psi)	4.83 (700)
Hold temperature, °C (°F)	593 (1100)
Low cycle temperature, °C (°F)	427 (800)
Hold time, h	160
Number of cycles	10
Material	Type 304 stainless steel

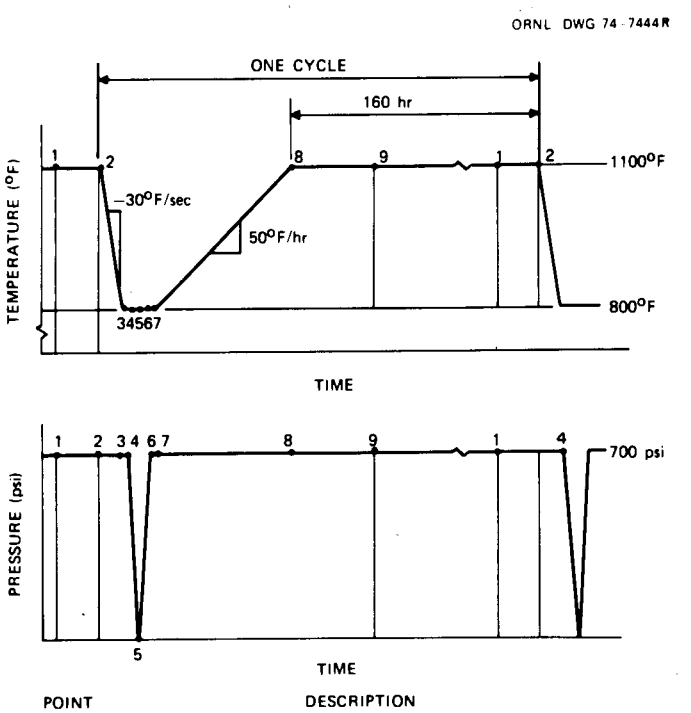

POINT	DESCRIPTION
1	~ ONE DAY BEFORE THERMAL TRANSIENT
2	BEGINNING OF THERMAL TRANSIENT
3	SPECIMEN REACHES UNIFORM 800°F
4	BEGINNING OF PRESSURE REMOVAL
5	ZERO PRESSURE
6	700 psi PRESSURE RESTORED
7	BEGINNING OF 50°F/hr TEMPERATURE INCREASE
8	BEGINNING OF STEADY-STATE OPERATION
9	AFTER 48 hr OF STEADY-STATE OPERATION

Fig. 2.1. Coolant temperature and pressure load histograms; T(°C) = [T(°F) − 32]/1.8; P(MPa) = 0.006895P (psi).

pipe is 35.91 $kW/m^2 \cdot K$ (43.92 $Btu/h \cdot in.^2 \cdot {}^\circ F$). After the thermal downshock, the coolant temperature is held at 427° C until the temperature in the pipe wall becomes uniform. The pipe is then depressurized, repressurized, reheated slowly to 593° C, and held at that temperature under load while creep occurs. Creep is not permitted during any part of the cycle except the hold periods.

3. MATERIAL PROPERTIES

As mentioned in Chapter 1, two types of analyses were performed in the present work—a design analysis and a series of sensitivity study analyses. The design analysis used only properties taken from the NSMH,[5] along with creep and fatigue data from CCN47.[6] The material properties that were used in the sensitivity study are presented in this chapter in their entirety. The data were obtained from 20 heats of type 304 stainless steel that were tested at four installations: Hanford Engineering Development Laboratory, Argonne National Laboratory, Babcock and Wilcox, and the Metals and Ceramics Division of Oak Ridge National Laboratory.

Material properties used in this work were in the form of equations or tables that specify the property as a function of temperature, stress, time, etc. The heat-to-heat variability of the properties was incorporated by introducing additional parameters into the equations. As an illustration, the monotonic or virgin yield stress used in the present work can be represented by the equation

$$\sigma_{y_o} = 20{,}400 - 8.5322\,T + 1{,}295\,A_{\sigma_y}\,. \tag{1}$$

where

σ_{y_o} = yield stress (psi), [σ_{y_o} (MPa) = 0.006895 σ_{y_o} (psi)],

T = temperature (° F), {T(° C) = [T(° F) − 32]/ 1.8},

A_{σ_y} = correction for heat-to-heat variability (dimensionless).

When dealing with known well-defined heats, A_{σ_y} is a known number; when dealing with unknown heats, A_{σ_y} must be treated as a random variable. Then the numerical value of A_{σ_y} is not known, but the statistical distribution of A_{σ_y} can still be determined, that is, the probability that A_{σ_y} lies in some range [e.g., (−2,+2)] can be established by the study of a large number of heats. In Eq. (1), A_{σ_y} was found to have a mean value of zero and a standard deviation of 1.0. Although the random variable in Eq. (1) appears in a simple additive term, a more complicated functional dependence is also possible, and more than one random variable can be introduced into an equation if necessary. [For example, if the slope of a plot of σ_{y_o} vs T showed a significant heat-to-heat variability, then an additional term in the form of a product $B_{\sigma_y}T$ could be introduced into Eq. (1), where B_{σ_y} is another random variable.]

The material property correlations used in the sensitivity study of the present work were taken from a report by McAfee and Sartory.[9] Readers interested in the data base or a discussion of the development of the equations should refer to that source. Only a listing of the correlations in the form in which they were used is provided here. For those properties for which Ref. 9 provided no results, the NSMH[5] data were used.

Creep strain

The creep strain at 593° C (1100° F) was specified by Ref. 9 through the following equations:

$$\epsilon^c = A_1(1 - e^{-R_1 t}) + A_2(1 - e^{-R_2 t}) + A_3(1 - e^{-R_3 t}) + 0.01\dot{\epsilon}_m t\,,$$

where

ϵ^c = creep strain (m/ m),

t = time (h),

$A_1 = (5.933 \times 10^{-6})\ \sigma(C/C^*)$,

$A_2 = (8.3524 \times 10^{-6})\ \sigma^{1.8768}\ C/C^*$,

$A_3 = (2.849 \times 10^{-7})\ \sigma^{3.6966}\ C/C^*$,

$R_1 = (9.4045 \times 10^{-2})\ e^{0.214454\sigma}\ (p/p^*)$,

$R_2 = (2.74945 \times 10^{-3})\ e^{0.17537\sigma}\ (p/p^*)$,

$R_3 = (1.0928 \times 10^{-4})\ e^{0.11757\sigma}\ (p/p^*)$,

$\dot{\epsilon}_m = (1.45649 \times 10^{-16})\ \sigma^{9.70335}\ (10^{0.56634A_{cr}})$,

$\dot{\epsilon}_m^* = (2.3206 \times 10^{-16})\ \sigma^{9.70335}$,

$t_r = 16.9256\ (\dot{\epsilon}_m)^{-0.7639}$,

$t_r^* = 16.9256\ (\dot{\epsilon}_m^*)^{-0.7639}$,

$C^* = 0.685\ (1.11\ \dot{\epsilon}_m^{*0.974} - \dot{\epsilon}_m^*)\ t_r^{*0.968}$,

$p^* = (3.43\ \dot{\epsilon}_m^{*0.8} - \dot{\epsilon}_m^*)/C^*$,

$C = 0.685\ (1.11\ \dot{\epsilon}_m^{0.974} - \dot{\epsilon}_m)\ t_r^{0.968}$,

$p = (3.43\ \dot{\epsilon}_m^{0.8} - \dot{\epsilon}_m)/C$,

σ = stress (ksi), [σ (MPa) = 6.895 σ (ksi)],

A_{cr} = random variable of zero mean and unit standard deviation which corrects the equation for heat-to-heat variability.

Thermal expansion

Based on NSMH data,[5] the thermal expansion was characterized by

$$\ell = 1.0 + (0.756084 \times 10^{-5}\ T) + (0.354815 \times 10^{-8}\ T^2) - (0.14397 \times 10^{-11}\ T^3) + (0.259441 \times 10^{-15}\ T^4)\ ,$$

where

ℓ = length of a specimen in arbitrary units,

T = temperature (° F), {T(° C) = [T(° F) − 32]/ 1.8}.

The instantaneous thermal expansion coefficient is related to ℓ by

$$\alpha = (1/\ell)(d\ell/dT)\ .$$

Elastic modulus

Based on data from the NSMH,[5]

$$E = (0.283367 \times 10^8) - (0.288221 \times 10^4\ T) - (0.369785 \times 10^1\ T^2) + (0.770919 \times 10^{-3}\ T^3)\ ,$$

where

E = Young's modulus (psi), [E (MPa) = (6.895×10^{-3}) E (psi)],

T = temperature (° F), {T(° C) = [T(° F) − 32]/ 1.8} .

Poisson's ratio

Based on NSMH data,[5]

$$\nu = 0.25964 + (0.626822 \times 10^{-4}\ T) - (0.292836 \times 10^{-7}\ T^2) + (0.11567 \times 10^{-10}\ T^3)\ ,$$

where

ν = Poisson's ratio,

T = temperature (° F), {T(° C) = [T(° F) − 32]/ 1.8} .

Yield stress

Based on the recommendations in Ref. 9 and from Corum,[10] the yield stress was obtained by adding 1295* A_{σ_y} to the value obtained by linear interpolation from Table 3.1. In Table 3.1,

$$\bar{\epsilon}^p = \int \left(\frac{2}{3}\ d\epsilon^p_{ij}\ d\epsilon^p_{ij}\right)^{1/2},$$

$$\bar{\epsilon}^c = \int \left(\frac{2}{3}\ d\epsilon^c_{ij}\ d\epsilon^c_{ij}\right)^{1/2},$$

$d\epsilon^p_{ij}$ = differential plastic strain tensor (m/ m),

$d\epsilon^c_{ij}$ = differential creep strain tensor (m/ m),

A_{σ_y} = random variable with zero mean and unit standard deviation that corrects the tabular result for heat-to-heat variability.

In the case of the virgin yield stress ($\bar{\epsilon}_p = \bar{\epsilon}_c = 0$), the yield stress obtained using Table 3.1 is identical to that obtained from Eq. (1). The quantity κ of RDT Standard F9-5T[11] is related to the yield stress σ_y

*The constant 1295 is in psi; 1295 psi = 8.929 MPa.

Table 3.1. Yield stress

$\bar{\epsilon}^p + \bar{\epsilon}^c$ (m/ m)	Temperature (° F)[a]			
	800	900	1000	1100
0	13,575[b]	12,721	11,868	11,015
0.005	13,632	13,423	12,130	12,279
0.01	14,047	13,911	12,808	13,168
0.02	14,598	14,518	13,700	14,361
0.03	14,943	14,922	14,260	15,251
0.04	15,208	15,243	15,676	15,953
0.05	15,415	15,541	15,009	16,432
0.058	15,472	15,696	15,140	16,467
1.0	15,472	15,696	15,140	15,467

[a] T(° C) = [T(° F) − 32]/ 1.8.
[b] Stresses are given in psi; σ_y (MPa) = 0.006895 σ_y (psi).

above by

$$\kappa = (\sigma_y^2)/3 .$$

Hardening coefficient

Based on Ref. 9, the mean value of the hardening coefficient was selected by setting

$$d\bar{\epsilon}^p/d\bar{\sigma} = [(1.4303 \times 10^{-4})\,(\mathrm{MPa})^{-1}][(0.98619 \times 10^{-6})(\mathrm{psi})^{-1}] ,$$

where

$$\frac{d\bar{\epsilon}^p}{d\bar{\sigma}} = \frac{E - E^p}{EE^p} ,$$

E = elastic modulus,

E^p = slope of the elastic-plastic portion of the bilinearized stress-strain diagram.

Note that the quantity C defined in RDT Standard F9-5T[11] is related to $d\bar{\epsilon}^p/p\bar{\sigma}$ by

$$C = \frac{2}{3(d\bar{\epsilon}^p/d\bar{\sigma})} .$$

Volumetric heat capacity

Based on NSMH data,[5]

$$\rho C_p = (0.320832 \times 10^{-1}) + (0.154792 \times 10^{-4}\,T) - (0.122301 \times 10^{-7}\,T^2) + (0.395032 \times 10^{-11}\,T^3) ,$$

where

ρC_p = volumetric heat capacity (Btu/in.^{3}·°F)

[ρC_p (MJ/m^3·K) = 115.8 ρC_p (Btu/in.^{3}·°F)],

T = temperature (°F), {T(°C) = [T(°F) − 32]/1.8}.

Thermal conductivity

Based on NSMH data,[5]

$$k = 0.680669 + (0.487159 \times 10^{-3}\,T) - (0.912897 \times 10^{-7}\,T^2) + (0.208299 \times 10^{-10}\,T^3) ,$$

where

k = thermal conductivity (Btu/in.·°F), [k (W/m·K) = 20.75 k (Btu/in.·h·°F)],

T = temperature (°F), {T(°C) = [T(°F) − 32]/1.8}.

Creep damage

The creep rupture time at 593° C (1100° F) was given by Ref. 9 as

$$t_r = 16.9256\,(\dot{\epsilon}_m)^{-0.7639}\,10^{0.17155 A_{t_r}}\,,$$

where

$$\dot{\epsilon}_m = (1.45649 \times 10^{-16})\,\sigma^{9.70335}\,10^{0.56634 A_{cr}}\,,$$

t_r = creep rupture time (h),

σ = stress (ksi), [σ (MPa) = 6.895 σ (ksi)],

A_{cr} = the same random variable of zero mean and unit standard deviation that was introduced in the creep equation,

A_{t_r} = a new random variable of zero mean and unit standard deviation.

Fatigue damage

The cyclic life, following the recommendation of Ref. 9 and Diercks and Raske,[12] was taken as

$$(\log_{10} N_f)^{-1/2} = 1.2055 + 0.6600\,S + 0.1804\,S^2 - 0.008143\,S^4 + 0.000253\,RS^4 + 0.000218\,T'S^4 - 0.0005466\,RT'^2\,,$$

where

N_f = cycles to failure,

$S = \log_{10}(\Delta\epsilon_t/100)$,

$R = \log_{10}(\dot{\epsilon})$,

$T' = T/100$,

$\Delta\epsilon_t$ = total strain range (%),

$\dot{\epsilon}$ = total strain rate (s^{-1}),

T = temperature (° C), {T(° C) = [T(° F) − 32]/ 1.8}.

Throughout the present sensitivity study,

$$\dot{\epsilon} = (0.33 \times 10^{-3})\,s^{-1}\,.$$

The above material property laws depend on three random variables: A_{cr}, A_{σ_y}, and A_{t_r}. If numerical values are assigned to these three parameters, then the values of the properties are defined, a complete structural analysis can be carried out, and all of the usual results of such an analysis can be calculated. Thus, every analysis result (e.g., the maximum creep damage after ten cycles) is a function of the three variables A_{cr}, A_{σ_y}, and A_{t_r}. In a later section, the results will be presented graphically in such a functional form. In Ref. 9, A_{cr}, A_{σ_y}, and A_{t_r} were all found to have a zero mean and a unit standard deviation, but their detailed distribution was not investigated. In this study, the assumption is that all three random

variables have a normal distribution. Such a distribution is completely determined by the values of its mean and standard deviation.

Reference 9 also indicated that the three random variables are statistically independent (uncorrelated). However, note that the random variable A_{cr} appears in both the creep equation and the creep rupture time. Thus, these two properties are strongly correlated, and a heat of material that has a higher-than-average linear creep rate is also likely to have a lower-than-average creep rupture time. The possibility of several such correlations between different material properties was examined in Ref. 9, but only the correlation between creep rate and creep rupture time was found to be significant.

Only three of the ten material property correlations presented above incorporate heat-to-heat variability parameters; they are the creep equation, the yield stress, and the creep rupture time. The three properties were selected on the basis of the availability of data and on judgment of their importance. In the case of fatigue damage cyclic life, however, Ref. 9 specifically recommends, on the basis of earlier work,[12] that no heat-to-heat variability be included.

4. STRUCTURAL ANALYSIS AND DAMAGE EVALUATION

4.1 Finite-Element Procedure

The inelastic structural analyses of this report were performed with the finite-element program PLACRE,[13] which carries out creep calculations by an incremental initial strain method[14] and plastic calculations by an iterative tangent stiffness method.[15]

In this work, the structure was one dimensional, with the stress, strain, and temperature dependent on radius only. For such one-dimensional pipe wall problems, PLACRE uses a special three-node rectangular element shown in Fig. 4.1(a). The displacement field within this element is given by

radial displacement, $u = a + br$,

axial displacement, $v = cz$,

where a, b, and c are constants determined from the nodal deflections. The resulting strains are

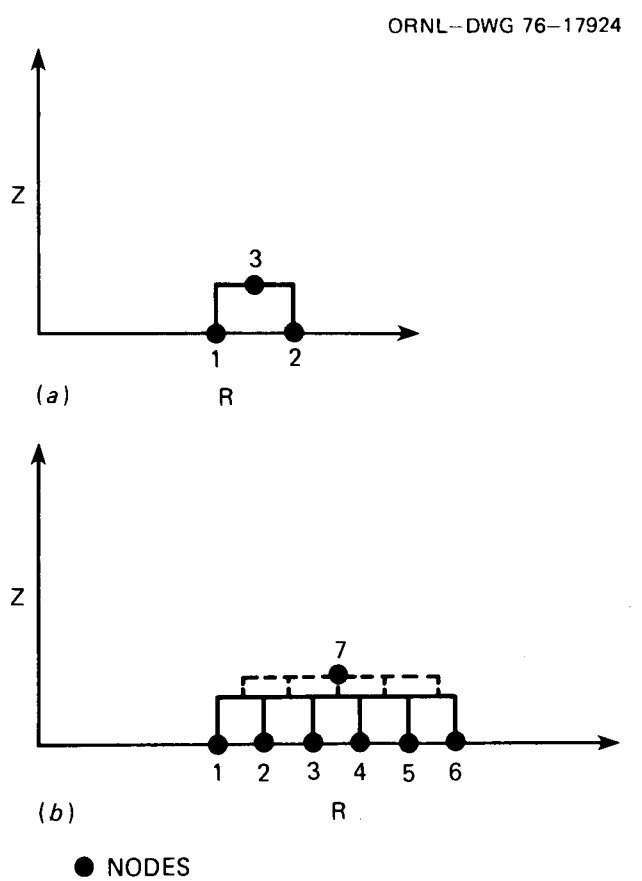

Fig. 4.1. PLACRE pipe-wall elements. (a) Illustration of a single three-node rectangular pipe-wall element; (b) arrangement of elements to simulate a pipe wall.

considered to be constant within each element and are given by

$$\epsilon_r = b \ ,$$

$$\epsilon_\theta = (a/\bar{r}) + b \ ,$$

$$\epsilon_z = c \ ,$$

$$\gamma_{rz} = 0 \ ,$$

where $\bar{r}$ is the constant mean radius of the element. This element does not include shear stress or strain, so only a purely axial load can be applied to node 3 of Fig. 4.1(a). Similarly, only a purely radial load can be applied to nodes 1 and 2.

To analyze a pipe wall, a single row of these rectangular elements was connected to a common upper node [Fig. 4.1(b)] to give generalized plane strain. Sixteen equally spaced elements were used through the thickness of the wall in this study.

4.2 Thermal Analysis Procedure

Temperature profiles needed as input to the structural analysis were calculated by PLACRE using a finite-difference procedure of the Crank-Nicholson[16] type. One node of the thermal finite-difference grid was located at the center of each structural finite element, and one additional node was used at each end of the grid as an aid in applying the boundary conditions. A heat transfer coefficient of 35.91 $kW/m^2 \cdot K$ (43.92 $Btu/h \cdot in.^2 \cdot {}^\circ F$) was applied between the sodium and the inner surface of the pipe wall. The outer surface of the pipe wall was considered insulated.

4.3 Constitutive Equations

The procedure for describing plastic and creep behavior used in this study was consistent with those recommended in RDT Standard F9-5T[11] and modified in Ref. 10.

Both the initial yield surface and the subsequent plastic loading surfaces were described by an equation of the von Mises form:

$$f = \frac{1}{2} (\sigma'_{ij} - \alpha_{ij}) (\sigma'_{ij} - \alpha_{ij}) = \kappa(\bar{\epsilon}^p + \bar{\epsilon}^c, T) \ ;^*$$

and, during plastic loading, the center α_{ij} of the yield surface was shifted according to

$$d\alpha_{ij} = \frac{S_{ij}}{2\kappa} [S_{k\ell} (d\sigma_{k\ell} - H d\epsilon^c_{k\ell}) - d\kappa] + H d\epsilon^c_{ij} \ ,$$

where $d\kappa$ is the total differential of κ due to all sources, and the plastic strain increment was given by

*For the design analysis, $\kappa = \kappa_0(T)$ was used for the initial load and $\kappa = \kappa_1(T)$ was used after the first incipient reverse plastic loading or after the accumulation of 0.2% effective creep strain, whichever occurred first.

$$d\epsilon^p_{ij} = \frac{S_{ij}}{2C_\kappa} \left[S_{k\ell} \left(d\sigma_{k\ell} - H d\epsilon^c_{k\ell} \right) - \frac{\partial \kappa}{\partial T} dT - \frac{\partial \kappa}{\partial \bar{\epsilon}^c} d\bar{\epsilon}^c \right],$$

where S_{ij} is equal to $\sigma'_{ij} - \alpha_{ij}$. The prime indicates the deviatoric part* of σ_{ij}.

In the absence of plastic loading, α_{ij} was shifted according to

$$d\alpha_{ij} = H d\epsilon^c_{ij} .$$

The hardening coefficients C and H were given by

$$C = \frac{2}{3(d\bar{\epsilon}^p / d\sigma)},$$

$$H = \begin{cases} C \text{ if } \bar{\alpha} \equiv [(3/2)\, \alpha_{ij}\, \alpha_{ij}]^{1/2} \leqslant A\sqrt{3\kappa}, \\ 0 \text{ if } \bar{\alpha} > A\sqrt{3\kappa}. \end{cases}$$

The value A = 0.3 that is recommended in Ref. 10 was adopted.

The plastic strain path length $\bar{\epsilon}^p$ and the creep strain path length $\bar{\epsilon}^c$ were defined by

$$\bar{\epsilon}^p = \int \left(\frac{2}{3}\, d\epsilon^p_{ij}\, d\epsilon^p_{ij} \right)^{1/2},$$

$$\bar{\epsilon}^c = \int \left(\frac{2}{3}\, d\epsilon^c_{ij}\, d\epsilon^c_{ij} \right)^{1/2}.$$

Creep behavior was described in PLACRE by an equation-of-state formulation using strain hardening. The creep strain increment was given by

$$d\epsilon^C_{ij} = \frac{3}{2} \frac{\dot{\bar{\epsilon}}^c(\bar{\sigma}, \bar{\epsilon}^H)}{\bar{\sigma}} \sigma'_{ij}\, dt,$$

where $\dot{\bar{\epsilon}}^c$ is the effective creep strain rate obtained from uniaxial data, $\bar{\sigma}$ is the effective stress $\bar{\sigma} = \sqrt{(3/2)\sigma'_{ij}\sigma'_{ij}}$, $\bar{\epsilon}^H$ is a modified effective total† creep strain, and dt is the time increment. In the case of monotonic creep, $\bar{\epsilon}^H$ is the effective total creep strain,

$$\bar{\epsilon}^H = \sqrt{(2/3)\epsilon^c_{ij}\, \epsilon^c_{ij}}.$$

In the case of creep under cyclic loading, special rules based on the loading history[11] have been established for determining $\bar{\epsilon}^H$. The cyclic creep rules of Ref. 11 were used in this work, although nearly the same results would likely be obtained with ordinary strain hardening because of the small amount of creep cycling occurring in the present analyses.

---

*The deviatoric components are defined as $\sigma_{ij} = \sigma_{ij} - 1/3\, \sigma_{kk}\delta_{ij}$.

†Total creep strain means the sum of the primary and secondary creep strains. (Some strain-hardening procedures use only the primary creep strain for hardening.)

4.4 Damage Evaluation

Creep rupture damage was evaluated in the usual way by calculating the integral

$$\int_0^t \frac{dt}{t_r},$$

where t is time and t_r is the creep rupture time at the calculated effective stress level divided by K′.

For design purposes, the calculated effective stress is usually divided by a constant $K' < 1.0$ before evaluating the creep rupture time t_r to ensure conservatism.[6] In the heat-to-heat variability sensitivity study of the present work, conservatism was not desired, and K was set to 1.0. In the design analysis based on current code recommendations, however, $K' = 0.9$ was used as usual. The damage integrals were taken only over the creep hold periods.

For the fatigue damage evaluation, the total strain range was calculated by postprocessor according to

$$\Delta\epsilon_t = \max_i \max_j \frac{\sqrt{2}}{3}\Big[(\epsilon_{r_j} - \epsilon_{r_i} - \epsilon_{\theta_j} + \epsilon_{\theta_i})^2 + (\epsilon_{\theta_j} - \epsilon_{\theta_i} - \epsilon_{z_j} + \epsilon_{z_i})^2 + (\epsilon_{z_j} - \epsilon_{z_i} - \epsilon_{r_j} + \epsilon_{r_i})^2 + \frac{3}{2}(\gamma_{rz_j} - \gamma_{rz_i})^2\Big]^{1/2},$$

where the two maxima were taken over all calculated points of the cycle and ϵ_{r_j} is the r component of the total mechanical strain at point j of the cycle. The temperature used for the fatigue damage evaluation was the maximum cycle temperature in all cases.

5. SENSITIVITY STUDY, DESIGN ANALYSIS, AND THEIR RESULTS

5.1 Selection of Quantities to Be Tested for Conservation

A total of ten calculated quantities that are listed in Table 5.1 were chosen as results to be tested for conservatism in the present study. The first three are the through-the-wall-mean, linear, and peak inelastic ratchetting strain that are defined and for which limits are specified in CCN47 (Ref. 6). The fourth and fifth entries are the maximum creep damage and fatigue damage for which a limit is also specified in CCN47 (Ref. 6). The above five quantities were determined at the end of the ten cycles analyzed.

Table 5.1. Quantities chosen as results to be tested for conservatism

No.	Calculated result	Design limit
1	Mean strain after ten cycles	1%
2	Linear strain after ten cycles	2%
3	Peak strain after ten cycles	5%
4	Creep damage after ten cycles	1.0
5	Fatigue damage after ten cycles	1.0
6	Cyclic life based on mean strain	
7	Cyclic life based on linear strain	
8	Cyclic life based on peak strain	
9	Cyclic life based on creep damage	
10	Cyclic life based on fatigue damage	

The pipe considered in the present study would not be expected to fail in the ten cycles analyzed, which is typical of the design situation; that is, the designer normally would analyze the structure for a small fraction of its expected life and then extrapolate to determine the allowable life. Extrapolation to the end of life has also been carried out in the present study. The mean, linear, and peak inelastic ratchetting strain were extrapolated linearly through the ninth and tenth cycles to the limits of 1, 2, and 5%, respectively, that are specified in CCN47 (Ref 6) and are listed in Table 5.1. This extrapolation results in three different cyclic lifetimes that are listed as entries six, seven, and eight in Table 5.1.

The situation for damage is more complicated because CCN47 does not specify separate limits for creep and fatigue damage but specifies a single envelope in which the damage must lie. If the damage envelope were used in this study to determine a single creep-fatigue lifetime, the result would be very insensitive to fatigue damage (which turns out to be much smaller than creep damage in this study). The extrapolated fatigue damage could then be significantly nonconservative without producing nonconservatism in the creep-fatigue lifetime. To avoid this possibility, separate creep and fatigue lifetimes were defined by setting a limit of 1.0 for both the creep and fatigue damage separately. The creep and fatigue lifetimes, which are listed as the ninth and tenth entries in Table 5.1, were then tested separately for conservatism.

5.2 Selection of Analysis Points and Details of Interpolation Procedure

The objective of the sensitivity study was to determine how the ten results of Sect. 5.1 vary with different heats, which were defined by assigning numerical values to the three random variables A_{cr}, A_{σ_y}, and A_{t_r} that enter into the material property correlations. After different values were chosen for these three random variables, an analysis was carried out at each selected point to establish the results. For the special case of A_{t_r}, however, because of the simple way t_r was used in the calculation of creep damage and the simple way A_{t_r} entered the correlation for t_r, it was only necessary to perform a finite-element analysis and creep damage evaluation for $A_{t_r} = 0$ and then multiply the result by $10^{-0.17155 A_{t_r}}$ to correct the creep damage for any other value of A_{t_r}. For the other two random variables, it was necessary to select a region in the (A_{cr}, A_{σ_y}) plane for study and then to select a set of points within the region for numerical calculations.

However, because the random variables are assumed to have a normal distribution regardless of what region is chosen for study, there is always some small probability that a heat will lie outside the range. Based on the time available for this study and given the uncertainty of what nonconservatism probabilities were of interest, it was decided to carry out analyses at a total of 16 points covering a range of (−2,+2) for both A_{cr} and A_{σ_y}. [With the normal distribution used in the present work, the value of A_{cr}, for example, lies within the interval (−2,+2) for about 95% of the heats.] Two-way interpolation by Chebyshev polynomials[17] was used to establish the results at points of the region of interest other than those selected for numerical calculation. Thus, the calculations were made at the zeros of the fourth-degree Chebyshev polynomial normalized to the range (−2,+2). The values of A_{cr} and A_{σ_y} used in the 16 cases analyzed are given in Table 5.2.

After a result (e.g., the creep damage after ten cycles) was calculated at the 16 points listed in Table 5.2, the logarithm was taken, and a two-way expansion in Chebyshev polynomials was determined. As described in a later section, millions of interpolations were necessary for the present work, and the cubic

Table 5.2. Values of the random variables chosen for analysis

Case	A_{cr}	A_{σ_y}
1	1.847759	1.847759
2	0.76536687	1.847759
3	−0.76536687	1.847759
4	−1.847759	1.847759
5	1.847759	0.76536687
6	0.76536687	0.76535587
7	−0.76536687	0.76536687
8	−1.847759	0.76536687
9	1.847759	0.76536687
10	0.76536687	−0.76536687
11	−0.76536687	−0.76536687
12	−1.847759	−0.76536687
13	1.847759	−1.847759
14	0.76536687	−1.847759
15	−0.76536687	−1.847759
16	−1.847759	−1.847759

expansion seemed excessively cumbersome. Therefore, an equally spaced rectangular grid of 529 (23 by 23) points was established over the square region $A_{cr} = (-2,+2)$, $A_{\sigma_y} = (-2,+2)$, and the Chebyshev expansion was used to establish the result at each of the 529 points. Thereafter, two-way linear interpolation on the 23 by 23 grid was used to evaluate the result. Linear extrapolation on the 23 by 23 grid was used outside the range of the grid. Both stages of interpolation were done on the logarithm of the result, so the antilogarithm was taken after interpolation.

5.3 Results of Sensitivity Study

As mentioned previously, results of the present sensitivity study (such as the calculated ratchetting strain) are functions of the three parameters A_{cr}, A_{σ_y}, and A_{t_r}, but A_{t_r} affects only creep damage. Thus, the through-the-wall-mean, linear, and peak ratchetting strain at the end of the tenth cycle can be represented by contour plots in the (A_{cr}, A_{σ_y}) plane, as shown in Figs. 5.1 through 5.3. The three plots are qualitatively very similiar, with the contours resembling quarter circles. The sensitivity of the ratchetting strain to changes in yield strength decreases as the yield strength increases; similarly, the sensitivity to changes in creep strength decreases as the creep strength increases (as A_{cr} decreases).

A contour plot of the creep damage after ten cycles for $A_{t_r} = 0$ is presented in Fig. 5.4.* This quantity primarily depends on A_{cr}, which influences both the creep rate and the creep rupture time, and

*The element number that gave the maximum creep damage was found to vary in a complicated manner as the parameters A_{cr} and A_{σ_y} were varied. In the majority of cases, an element interior to the wall gave the most damage. In this work, the element giving the greatest creep damage was used to set the maximum damage for the structure, and no interpolation or extrapolation from element to element was used. Conversely, in the case of peak ratchetting strain and fatigue damage strain range, extrapolation to the surface was used.

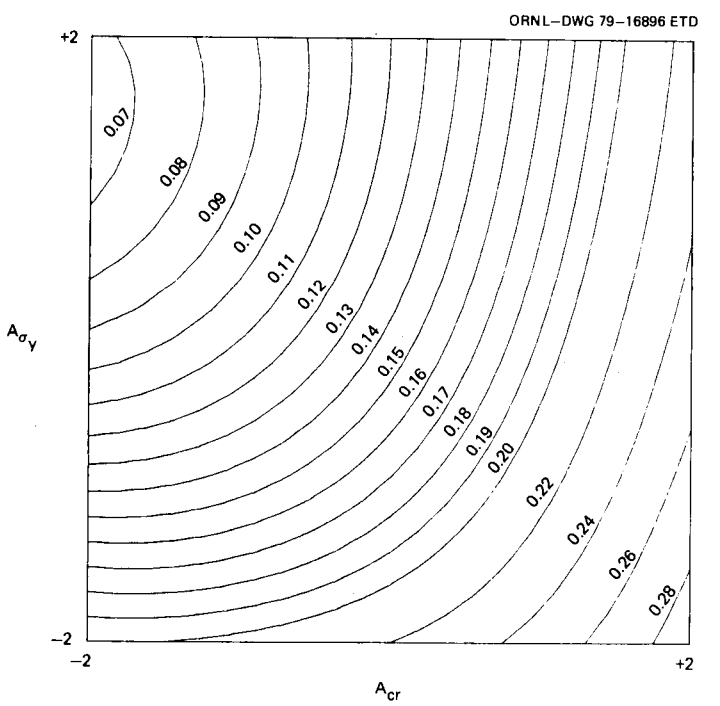

Fig. 5.1. Contours of constant mean inelastic ratchetting strain after ten cycles plotted in (A_{cr}, A_{σ_y}) plane. Labels on contours are in percent strain. Diagram covers ±2 standard deviations for both A_{cr} and A_{σ_y}.

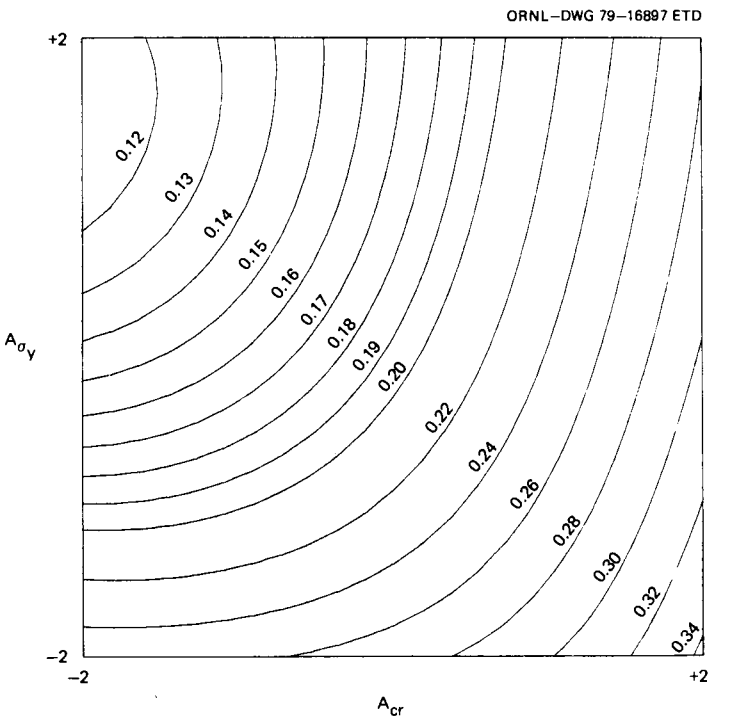

Fig. 5.2. Contours of constant linear inelastic ratchetting strain after ten cycles plotted in (A_{cr}, A_{σ_y}) plane. Labels on contours are in percent strain. Diagram covers ±2 standard deviations for both A_{cr} and A_{σ_y}.

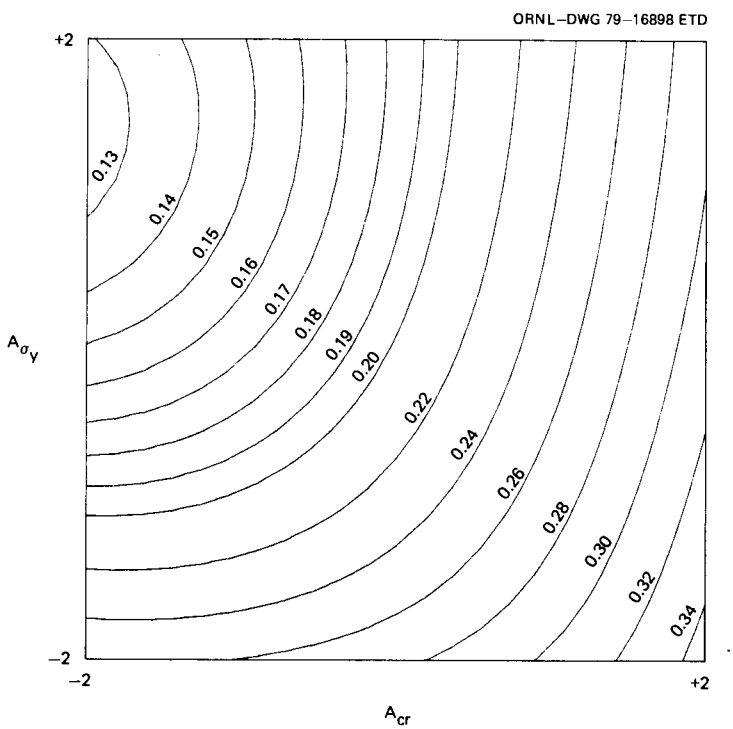

Fig. 5.3. Contours of constant peak inelastic ratchetting strain after ten cycles plotted in (A_{cr}, A_{σ_y}) plane. Labels on contours are in percent strain. Diagram covers ±2 standard deviations for both A_{cr} and A_{σ_y}.

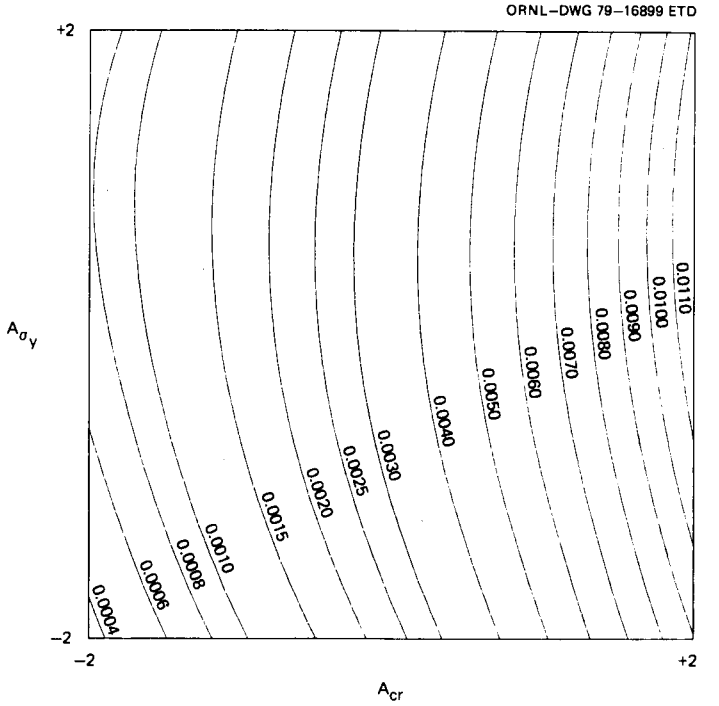

Fig. 5.4. Contours of constant creep damage fraction after ten cycles plotted in (A_{cr}, A_{σ_y}) plane. Diagram covers ±2 standard deviations for both A_{cr} and A_{σ_y}. Graphical result must be multiplied by $10^{-0.17155A_{t_r}}$.

a large value of A_{cr} indicates a large creep rate and a small creep rupture time. The rapid reduction in peak stress caused by stress redistribution at high creep rates is more than offset by the short creep rupture time that also accompanies the high creep rate. Thus, a large A_{cr} results in a large creep damage. Although Fig. 5.4 applies to $A_{t_r} = 0$, results for other values of A_{t_r} can be obtained simply by multiplying the results read from the graph by $10^{-0.17155A_{t_r}}$.

A contour plot for the fatigue damage after ten cycles is presented in Fig. 5.5. This quantity primarily depends on A_{σ_y}, so the contours are nearly horizontal.

Contour plots for the cyclic lifetimes based on the through-the-wall-mean, linear, and peak inelastic ratchetting strain are shown in Figs. 5.6 through 5.8. Again the three plots are similar to one another. The change in shape of the contours in going from the tenth cycle strain to the cyclic life based on the corresponding strain is surprising, however. Apparently, the effect of the extrapolation to the end of life depends significantly on the point chosen in the (A_{cr},A_{σ_y}) plane.

Plots of the cyclic lifetimes based on unit creep damage and unit fatigue damage are shown in Figs. 5.9 and 5.10. The contours qualitatively resemble those for the corresponding plots after ten cycles. The result presented in Fig. 5.9 must be multiplied by $10^{0.17155A_{t_r}}$ to correct for nonzero values of A_{t_r}.

5.4 Results of Design Analysis

As mentioned previously, this work included (for purposes of comparison) a design analysis that used the material properties from NSMH and damage data from CCN47 and that followed as closely as possible the procedures a designer might use, including the usual sources of conservatism. Results of the design analysis are most conveniently presented by tabulating the numerical values of the ten quantities of Table 5.1. This is done in Table 5.3.

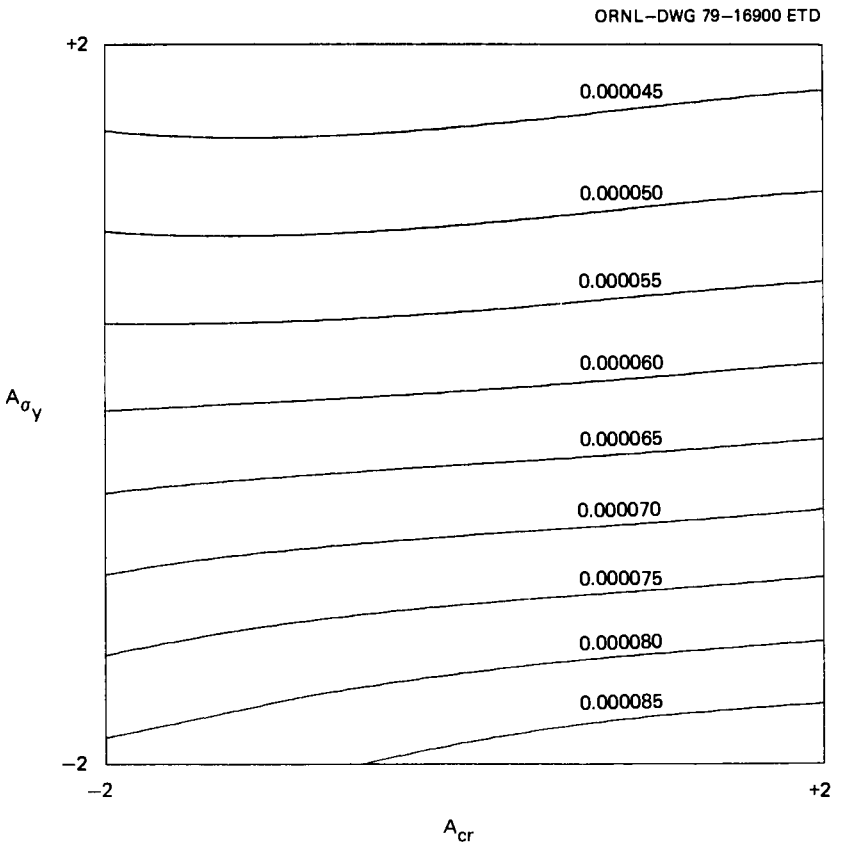

Fig. 5.5. Contours of constant fatigue damage fraction after ten cycles plotted in (A_{cr}, A_{σ_y}) plane. Diagram covers ±2 standard deviations for both A_{cr} and A_{σ_y}.

Table 5.3. Results of the design analyses

No.	Quantity	Value
1	Mean strain after ten cycles	0.114%
2	Linear strain after ten cycles	0.148%
3	Peak strain after ten cycles	0.164%
4	Creep damage after ten cycles	0.0210
5	Fatigue damage after ten cycles	0.0019
6	Cyclic life based on mean strain	197
7	Cyclic life based on linear strain	365
8	Cyclic life based on peak strain	900
9	Cyclic life based on creep damage	538
10	Cyclic life based on fatigue damage	5943

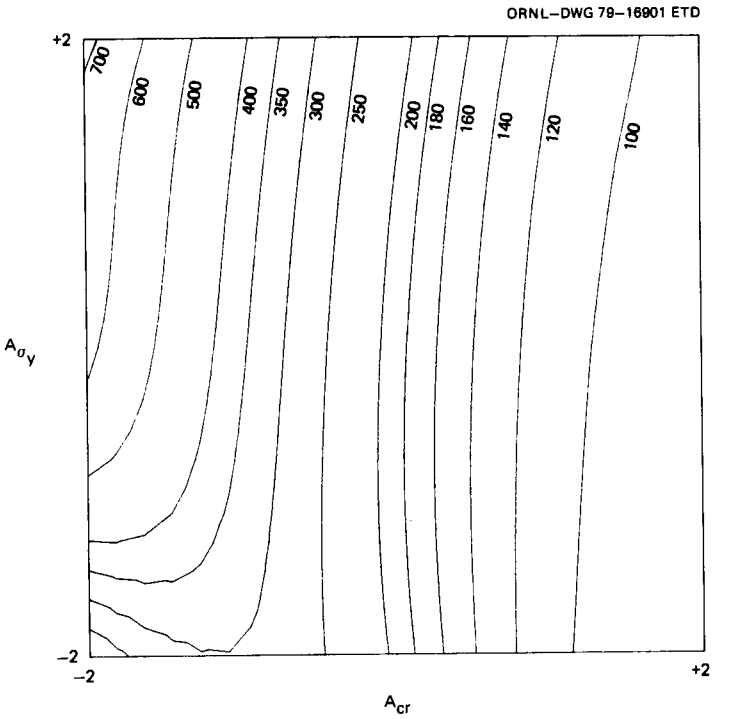

Fig. 5.6. Contours of constant cycles to 1% mean inelastic ratchetting strain plotted in (A_{cr}, A_{σ_y}) plane. Diagram covers ±2 standard deviations for both A_{cr} and A_{σ_y}.

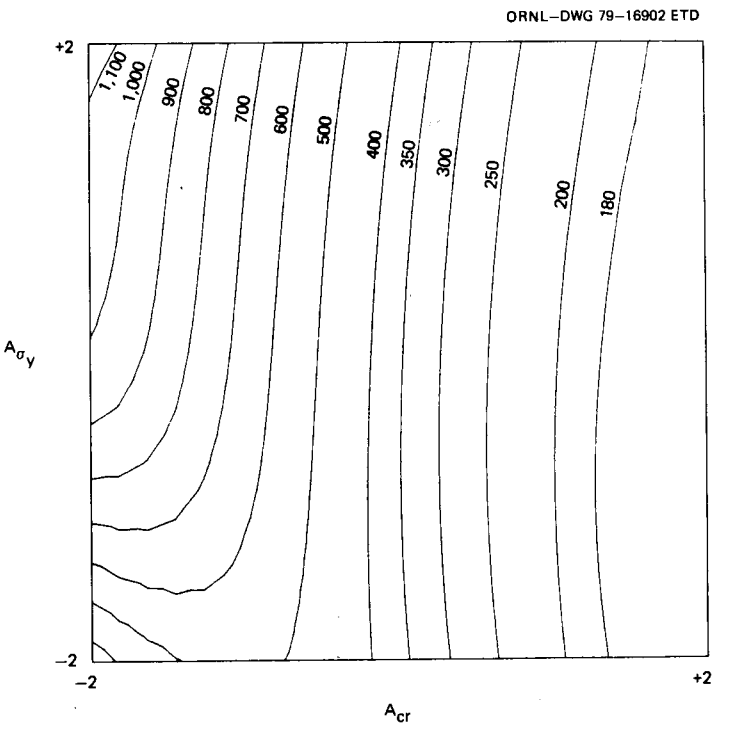

Fig. 5.7. Contours of constant cycles to 2% linear inelastic ratchetting strain plotted in (A_{cr}, A_{σ_y}) plane. Diagram covers ±2 standard deviations for both A_{cr} and A_{σ_y}.

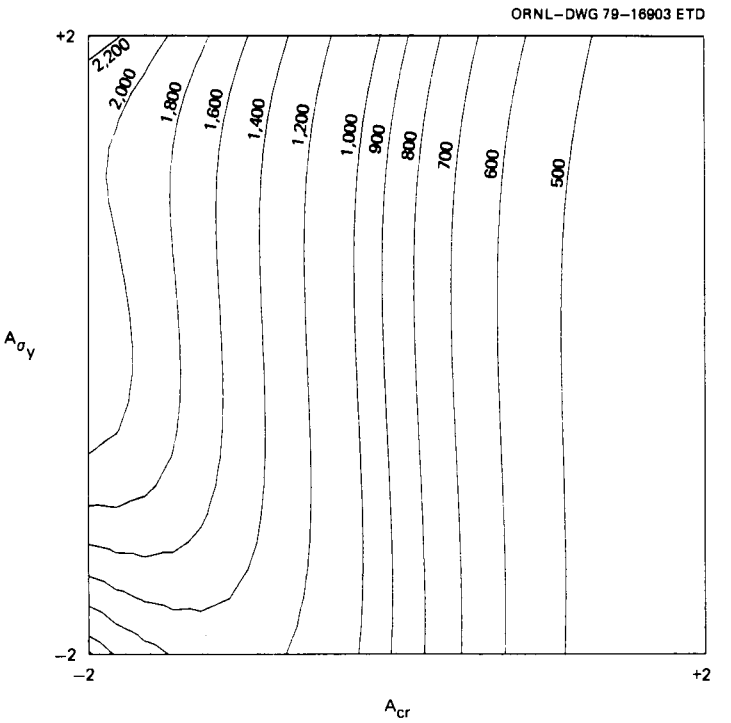

Fig. 5.8. Contours of constant cycles to 5% peak inelastic ratchetting strain plotted in (A_{cr}, A_{σ_y}) plane. Diagram covers ±2 standard deviations for both A_{cr} and A_{σ_y}.

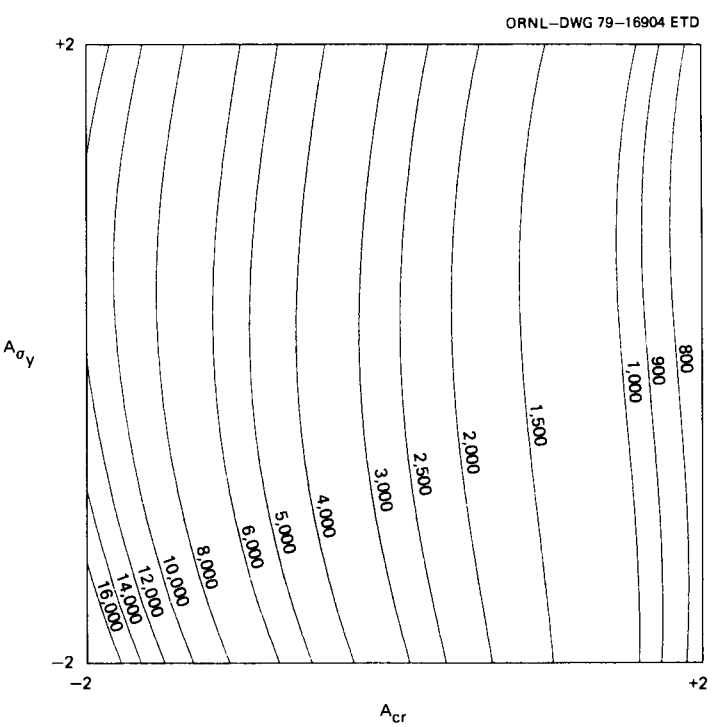

Fig. 5.9. Contours of constant cycles to unit creep damage fraction plotted in (A_{cr}, A_{σ_y}) plane. Diagram covers ±2 standard deviations for both A_{cr} and A_{σ_y}. Graphical result must be multiplied by $10^{0.17155A_{t_r}}$.

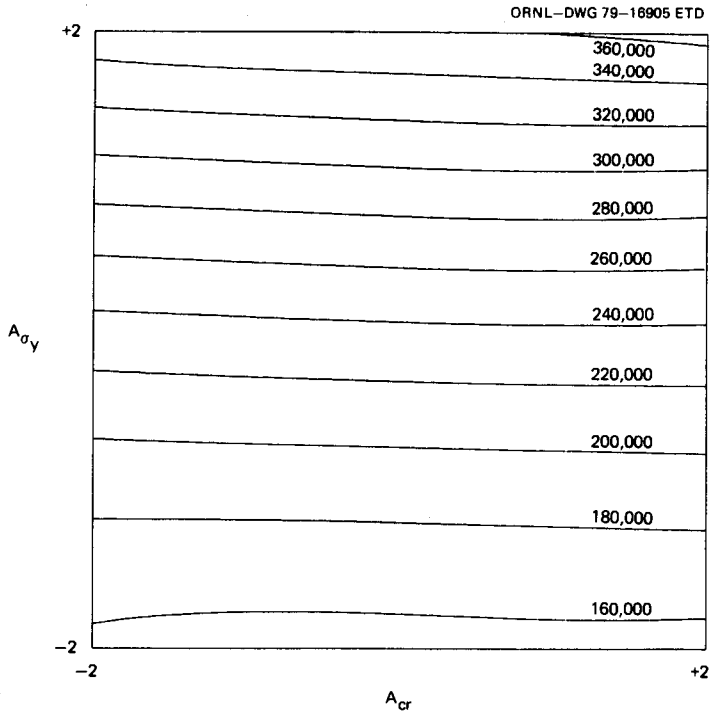

Fig. 5.10. Contours of constant cycles to unit fatigue damage fraction plotted in (A_{cr}, A_{σ_y}) plane. Diagram covers ±2 standard deviations for both A_{cr} and A_{σ_y}.

6. ANALYSIS OF CONSERVATISM AND ASSOCIATED RESULTS

Chapter 5 presented the results of the sensitivity study and the design analyses. Those results must now be used to evaluate the conservatism of the design procedures.

6.1 Technique Used to Determine Conservatism

To evaluate the conservatism of the design analyses, a Monte Carlo calculation was used which involved the following five steps.

1. Select a heat at random. This is done by computer generating three uncorrelated random numbers from a normal distribution with a zero mean and a unit standard deviation. These three random numbers are interpreted as the values of the three random variables A_{cr}, A_{σ_y}, and A_{t_r}. The numbers completely define the random heat for this study.

2. Interpolate from a table of sensitivity study results to obtain some specific quantity, for example, the cyclic life based on unit creep damage, for $A_{t_r} = 0$ and for the values of A_{cr} and A_{σ_y} selected above. (Use linear extrapolation if necessary.)

3. Correct the creep damage life, for example, for the randomly selected value of A_{σ_y} by multiplying by $10^{0.17155 A_{t_r}}$. This correction is not necessary for ratchetting strain, fatigue damage, or their associated lifetimes.

4. Compare the result for the randomly selected heat with the result obtained for the design analysis. If the ratchetting strain, creep damage, or fatigue damage for the random heat is greater or if the cyclic life based on ratchetting strain, creep damage, or fatigue damage for the random heat is smaller than the value obtained for the design analysis, then the design analysis is considered nonconservative. Otherwise, it is conservative.

5. Finally, repeat the above four steps for one million different randomly selected heats and count the cases that are nonconservative.

6.2 Results of Determination of Conservatism

The results of a count of the heats for which the design analysis is nonconservative are presented in Table 6.1.

Table 6.1. Percentage of heat for which design analysis is nonconservative

No.	Variable	Heats nonconservative (%)
1	Mean inelastic strain after ten cycles	81
2	Linear inelastic strain after ten cycles	89
3	Peak inelastic strain after ten cycles	87
4	Creep damage after ten cycles	0.54
5	Fatigue damage after ten cycles	0
6	Cyclic life based on 1% mean strain	52
7	Cyclic life based on 2% linear strain	51
8	Cyclic life based on 5% peak strain	52
9	Cyclic life based on 1.0 creep damage	1.8
10	Cyclic life based on 1.0 fatigue damage	0

Table 6.1 shows that, for the six quantities related to inelastic ratchetting strain, the design analysis is nonconservative for a majority of the heats. For the creep damage after ten cycles and the cyclic life based on unit creep damage, the design analysis is nonconservative for about 1% of the heats. For the fatigue damage after ten cycles and the cyclic life based on unit fatigue damage, the design analysis is conservative for all the one million heats.

6.3 Effect of Possible Added Safety Factors on Percentage of Nonconservatism

As shown in Table 6.1, the currently recommended design analysis is sometimes nonconservative. The question then naturally arises whether reducing or eliminating the nonconservatism is possible by introducing additional safety factors into the design procedures.

Safety factors or design margins can be incorporated in various ways and at various stages of the design procedure. The only type of added margin considered in this work is a simple constant factor that is (1) multiplied by the mean strain, linear strain, peak strain, creep damage, or fatigue damage after ten cycles or (2) divided into the corresponding cyclic lifetimes as calculated by the design analysis to produce a modified design result that replaces the design analysis result of Table 5.2. The modified result can then be compared directly with the result of a sensitivity analysis to evaluate a modified percentage nonconservatism. (However, the safety factor is not incorporated into the sensitivity analysis results.)

A range of added safety factors has been considered in this work, and the determination of nonconservatism described in Sects. 6.1 and 6.2 has been repeated. Results of the modified determination of nonconservatism are presented in Figs. 6.1 to 6.8, which show that an added safety factor of approximately 2 is required to reduce the percentage nonconservatism by an order of magnitude.

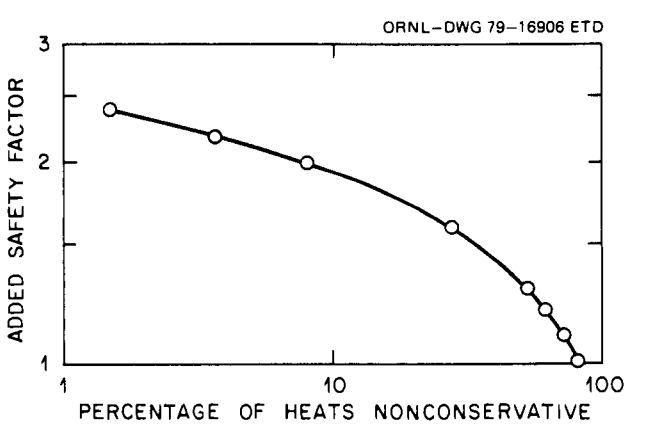

Fig. 6.1. Required added safety factor plotted as a function of desired percentage of nonconservatism for mean inelastic ratchetting strain after ten cycles.

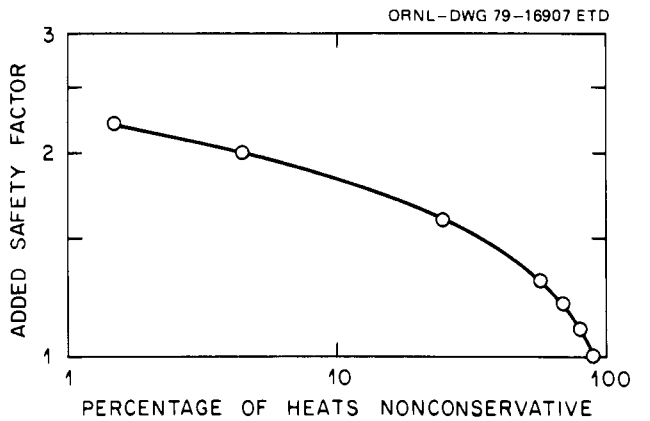

Fig. 6.2. Required added safety factor plotted as a function of desired percentage of nonconservatism for linear inelastic ratchetting strain after ten cycles.

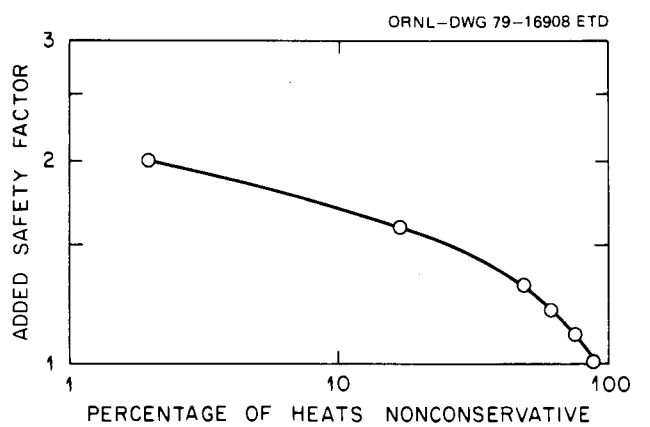

Fig. 6.3. Required added safety factor plotted as a function of desired percentage of nonconservatism for peak inelastic ratchetting strain after ten cycles.

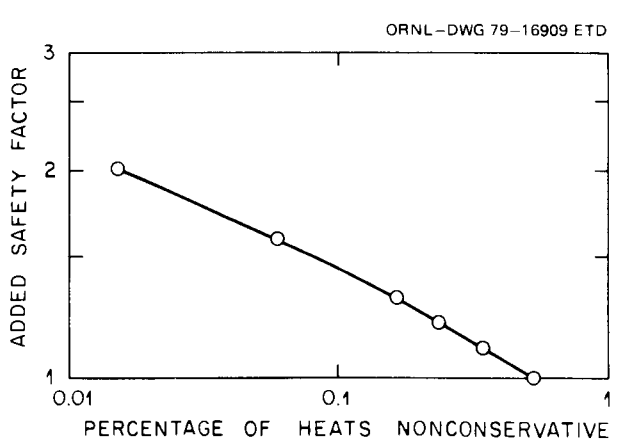

Fig. 6.4. Required added safety factor plotted as a function of desired percentage of nonconservatism for creep damage fraction after ten cycles.

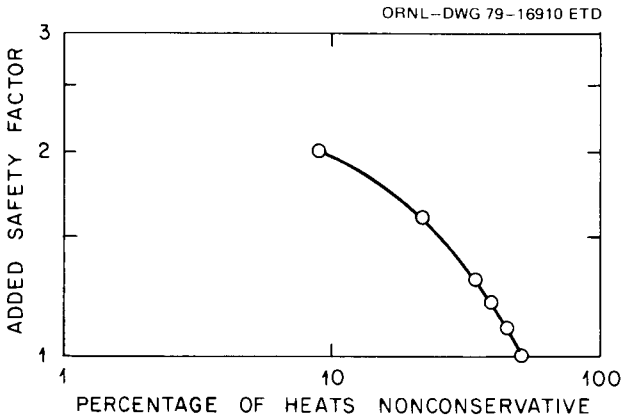

Fig. 6.5. Required added safety factor plotted as a function of desired percentage of nonconservatism for number of cycles to 1% mean inelastic ratchetting strain.

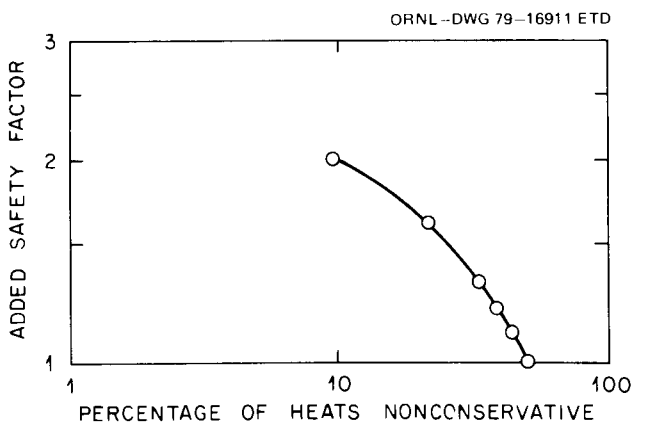

Fig. 6.6. Required added safety factor plotted as a function of desired percentage of nonconservatism for number of cycles to 2% linear inelastic ratchetting strain.

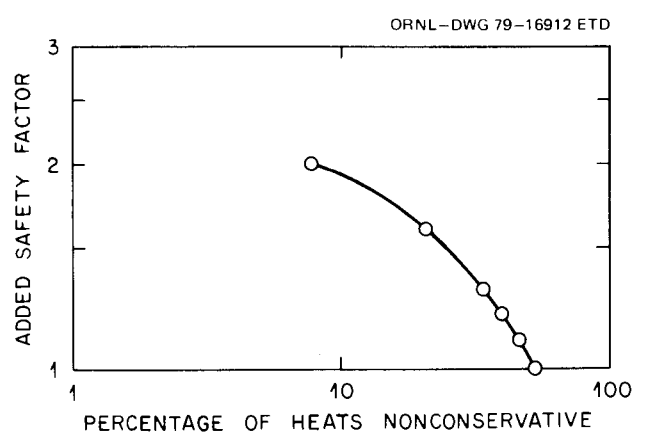

Fig. 6.7. Required added safety factor plotted as a function of desired percentage of nonconservatism for number of cycles to 5% peak inelastic ratchetting strain.

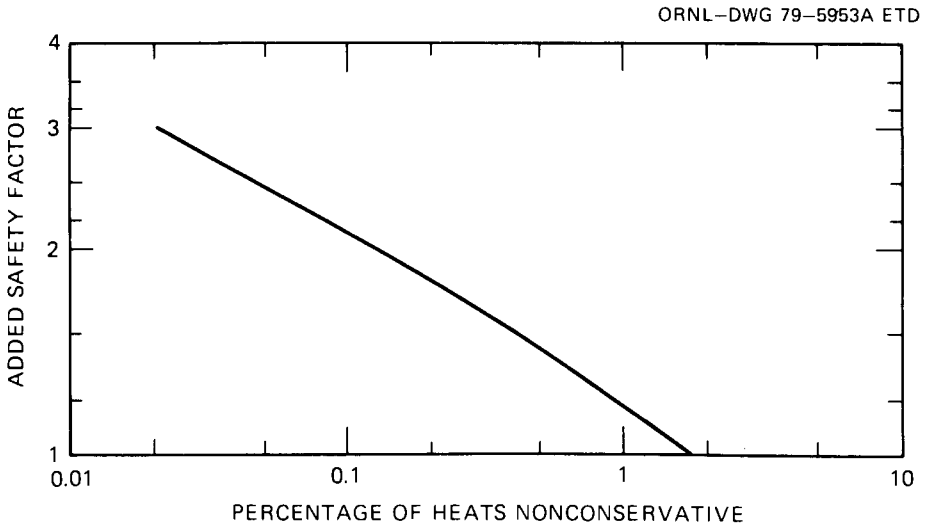

Fig. 6.8. Required added safety factor plotted as a function of desired percentage of nonconservatism for number of cycles to unit creep damage fraction.

7. DISCUSSION OF RESULTS

The percentages of nonconservatism reported in Table 6.1 are greatest for the ratchetting strain measures, much less for creep damage, and too small to detect for fatigue damage. In assessing the importance of these results, it is useful to examine the sources of design margin that are allowed for in this study. These sources are shown in Table 7.1.

Table 7.1. Sources of design margin for currently recommended design procedures incorporated into this study

Ratchetting strain	None!
Creep damage	Design curve is a minimum curve; in addition, calculated stress is divided by 0.9 before referring to design curve
Fatigue damage	Design curves are constructed by dividing cyclic life by 20 or strain range by 2, whichever is more conservative

Note that, in the case of ratchetting strain, no allowance is made for conservatism. Code Case N47 (Ref. 6) states, for example, that the maximum through-the-wall-mean inelastic ratchetting strain should be limited to 1%. The authors do not suggest that there is no conservatism in the 1% limit; however, the difficulty is that the precise degree of conservatism is not given by CCN47. If the statement was made, for example, that a 2% limit on mean strain was considered acceptable but that a 1% limit was being specified to ensure conservatism, the 2% limit could have been applied to the present sensitivity study and the 1% limit to the design analysis. Then a comparison between the resulting cyclic lifetimes would have incorporated the specified degree of conservatism. Because the degree of conservatism of the strain limits was unknown in the present work, no allowance was made for this. Thus, a calculation of a nonconservative strain for some heat is not necessarily equivalent to predicting failure or unacceptable performance of the structure for that heat.

For creep and fatigue damage, the code design margins are specified more clearly; in addition, there is likely to be more general agreement that a damage fraction of 1.0 (based on the true properties of the heat and without added conservatism) should not be exceeded. Thus, the results obtained for creep damage and creep life might be the most significant of this work.

The present work is based on a *statistical* treatment of nonconservatism. Such an approach seems reasonable in view of the random nature and wide scattering of creep rupture data, for example. Because a normal statistical distribution is assumed, reducing the probability or percentage of nonconservatism precisely to zero is impossible regardless of the choice of safety factor. (The tails of the Gaussian distribution extend to infinity and never drop all the way to zero.) Thus, the results presented in Sect. 6.3 take the form of graphs relating the additional required safety factor to the percentage of nonconservatism that is considered allowable or acceptable. Such graphs represent the most that can be deduced from a study of this type. Of course, establishing and recommending a specific safety factor to be used in design would be desirable; that would require the selection of a definite allowable probability of nonconservatism. However, the present work does not provide a basis for the selection of an allowable probability of nonconservatism. [A study of the consequences of nonconservatism (in terms of safety, economics, and politics) might provide such a basis.] Thus, this report stops short of recommending a definite safety factor.

This work deals solely with the consequences of heat-to-heat variability, which is only one of many possible sources of uncertainty or variability in the design procedure. The block diagram illustrated in Fig. 7.1 might help put this study in perspective. The top block in Fig. 7.1 is labeled "Structural Analyses Using Handbook Data" and represents the analysis carried out by the designer. The bottom block is labeled "Actual Structural Behavior." The designer must make some inferences about this behavior. For the purposes of this study, a third block is interposed that is labeled "Structural Analysis Using Actual Heat Data." By adding this intermediate block, the uncertainty or variability involved in inferring the actual structural behavior from the design analysis is divided into two contributions. The upper source of uncertainty is solely due to heat-to-heat variability and is the subject of this report. The lower source of uncertainty is due to all other causes and is beyond the scope of this report. Thus, recognize that when it is reported in Table 6.1 the design analysis is nonconservative with respect to creep damage life in 1.8% of the heats, what is really meant is that in 1.8% of the heats, the heat-to-heat variability is sufficient to use the entire design margin of CCN47, with no margin left for all other sources of uncertainty. If some code margins are required for other sources of uncertainty, then the percentage of nonconservatism must be greater than 1.8. Additional testing of structures to failure is desirable to assess the margin required for other sources of uncertainty.

Although this study is solely concerned with the consequences of heat-to-heat variability of material properties, it is not exhaustive even in that area because it limits the variability to only three of ten properties used in the analyses. The three properties were chosen, however, because they were believed to be the most important.

Five of the quantities listed in Table 5.1 as results of the present analyses are based on linear extrapolation from the ninth and tenth cycles to the end of life, as discussed in Sect. 5.1. The extrapolation of ratchetting strain to the end of life is discussed in RDT Standard F9-5T.[11] The

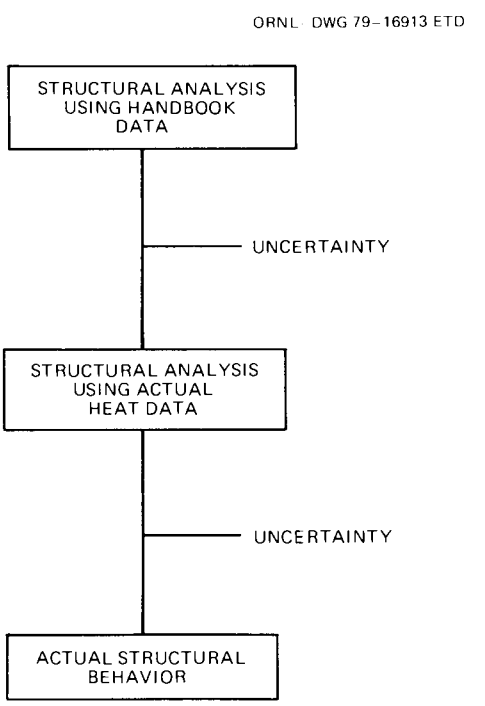

Fig. 7.1. Simple block diagram illustrating how the uncertainty in inferring actual structural behavior from a design analysis is divided into a contribution due to heat-to-heat variability and a contribution due to other sources.

standard states, "extrapolation to the end of life should be performed only when the results of the last three unit histograms show a consistent pattern of constant or decreasing strain accumulation per unit histogram."[11] No corresponding limitation is provided for the extrapolation of damage, but testing the results against the same criterion seems reasonable. In an earlier comparison between the results of elastic and inelastic design rules,[3] the observation was made that in many cases this criterion for extrapolability was not met even after ten cycles of inelastic analyses. In this work, for all three measures of ratchetting strain, the criterion for extrapolability was satisfied both in the design analysis and in all 16 cases of the sensitivity study. For creep damage, the criterion for extrapolability was satisfied for the design analysis; however, for 10 of the 16 cases of the sensitivity study, the incremental creep damage increased (usually by a few percent) during the last 3 cycles, so the criterion for extrapolability was not met. For fatigue damage, the criterion of extrapolability failed to be satisfied in the design analysis and in 1 of the 16 sensitivity study cases. In the most interesting case of creep damage where the extrapolability criterion was satisfied for the design analysis but not always for the sensitivity analyses, the cyclic life based on unit creep damage presumably could be smaller for the sensitivity analyses than indicated by present extrapolated results. Thus, the percentage of nonconservatism for this quantity could be larger than reported here due to this source.

In addition to the extrapolation to end of life, interpolation and extrapolation of the (A_{cr}, A_{σ_y}) plane was also required. The detailed procedure followed was described in Sect. 5.2. Excluding fatigue damage for which no nonconservatism was found, extrapolation played the most important role for creep damage and the associated cyclic life. No precise assessment of the errors of interpolation or extrapolation was carried out; however, to form a rough judgment of the validity of the extrapolation, a cross plot of creep life vs A_{cr} on semilogarithmic coordinates was constructed. (Note that the cyclic creep life most strongly depends on A_{cr}.) This plot was observed to be nearly linear, which lends some support to the linear extrapolation procedure that was followed. For the plots of ratchetting strain, the shape of the contours is more complicated, so the errors of interpolation or extrapolation are likely to be greater. For the cyclic life based on ratchetting strain, the contours are most complicated of all because they are nearly vertical over most of the figure but break sharply in one corner. In addition, the change of cyclic life with A_{cr} becomes very flat (sometimes the interpolated values even double back on themselves) to the right of the plot (for A_{cr} near +2). To minimize the extrapolation required in these cases, the plots of percent nonconservatism vs safety factor were terminated at a safety factor of 2.

Because only a small percentage of heats were found to lead to nonconservatism of the design analysis in the case of creep damage and cyclic life based on unit creep damage, the question arises as to whether these nonconservative heats are very peculiar in some way and, if so, in what way. To explore this question, all those heats (of the million heats drawn at random) that were marginally nonconservative (nonconservative by a margin of from 0 to 2%) with respect to cyclic life based on unit creep damage were segregated. There were 1107 marginally nonconservative heats. To typify these 1107 heats, a mean marginally nonconservative heat was determined by calculating the average values of the three random variables. These values were found to be $A_{cr} = 1.823$, $A_{\sigma_y} = 0.034$, and $A_{t_r} = -1.056$; that is, the mean marginally nonconservative heat had a creep strength that was nearly two standard deviations weaker than the mean of all heats, a yield strength that was nearly equal to the mean of all heats, and a time to rupture that fell about one standard deviation below the correlation between time to rupture and minimum creep rate. Determining the cycles to unit creep damage for the mean marginally nonconservative heat might be instructive. Referring to Fig. 5.9 and locating the point ($A_{cr} = 1.823$, $A_{\sigma_y} = 0.034$) on the plot with the aid of a ruler, the cyclic life is found to be about 800 cycles for $A_{t_r} = 0$. After multiplying by the required factor of $10^{-0.17155 A_{t_r}}$, the corrected cyclic life is about 527. From

Table 5.3, we find that the cyclic life based on unit creep damage for the design analysis is 538. Thus, the mean marginally nonconservative heat is barely nonconservative, as expected.

Although the 1107 marginally nonconservative heats have not been examined individually in detail, we can speculate on their distribution. Because Fig. 5.9 shows little effect of yield strength on the cycles to unit creep damage, the marginally nonconservative heats are expected to have a distribution of values of A_{σ_y} that is nearly the same as the distribution for all heats. The parameter A_{t_r} affects only the creep rupture time. In addition, the major effect of A_{cr} is also believed to be on the creep rupture time. Combining the effect of these two parameters, we find that the mean marginally nonconservative heat has a creep rupture time that is smaller by a factor of 0.113 than the mean for all heats. Of course, there are other combinations of A_{cr} and A_{t_r} that also give a creep rupture time of 0.113 of the mean, and we believe the values of A_{cr} and A_{t_r} for the individual marginally nonconservative heats lie roughly along such a tradeoff relationship. (There is a direct effect of creep strength on creep damage due to stress redistribution, as well as an indirect effect due to the statistical correlation between creep strength and rupture strength. The correlation between creep strength and rupture strength is believed to be the most important effect.)

If we examine the creep rupture data for the 20 heats on which this work is based,[9] the lowest individual time-to-rupture point lies below the mean curve for all data by a factor of 0.164. Thus, the mean marginally nonconservative heat in this study is slightly lower in creep rupture strength than the lowest point of the data base; no point in the data base is weak enough to indicate failure. There is some probability that if many more heats had been included in the data base, a few heats would have been found that were weaker than any in the present data base. Thus, points further below the mean curve than the factor 0.113 of the mean marginally nonconservative heat could occur.

In addition to the above study of the marginally nonconservative heats, the mean of all nonconservative heats (all heats that had a predicted cyclic creep life less than the design value of 538) was also determined. The average values of the random variables were found to be $A_{cr} = 2.096$, $A_{\sigma_y} = 0.047$, and $A_{t_r} = -1.275$. Comparing these values with those obtained above, the mean of all nonconservative heats is qualitatively very similar to the mean of marginally nonconservative heats, but each parameter is slightly farther from the center of the distribution.

In summary, an examination of the marginally nonconservative heats reveals that such heats lie along the side of the distribution corresponding to low creep strength and low creep rupture time, as would be expected, but they otherwise show no remarkable characteristics. The mean of all nonconservative heats also lies along the side of the distribution corresponding to low creep strength and low creep rupture time and lies somewhat farther from the center of the distribution than the mean of the marginally nonconservative heats but again shows no other remarkable characteristics.

8. SUGGESTIONS FOR FUTURE WORK

There are a number of extensions of this work that might be interesting to pursue.

Heat-to-heat variability was considered for only three of the ten material properties used in the analyses. Most of the other properties probably also exhibit some degree of heat-to-heat variability, and it would be interesting to know the resulting effect on the conservatism if all were considered. Unfortunately, even if sufficient data were available to specify the variability of all the properties, the difficulty of a study of the present type would increase rapidly if more random variables were added. One or two additional variables might be the limit of what could be done reasonably.

In addition to heat-to-heat variability, metals also exhibit significant specimen-to-specimen variability within a heat. The specimen-to-specimen variability seems worthy of further consideration both in the statistical analysis of the property data and the determination of the effect on structural behavior. The possible effect of specimen volume on specimen-to-specimen variability is not clear. A large structure (which could be considered to be made up of many smaller specimens of the size used for material property testing) could exhibit much less specimen-to-specimen variability than would be suggested by a statistical analysis of property data.

The interpolation and extrapolation procedures followed in the (A_{cr}, A_{σ_y}) plane were discussed in Sect. 5.2, and some limitations of the procedures were discussed in Chapter 7. Further investigation of the resulting error might be interesting. In particular, if a definite desired percentage of nonconservatism were established, a sensitivity study could be tailored to permit the establishment of the required factor of safety with a minimum of extrapolation in the (A_{cr}, A_{σ_y}) plane.

In applying the material property correlations in the present work, we assumed that the random variables A_{cr}, A_{σ_y}, and A_{t_r} were normally distributed. It would be desirable to carry out an analysis to determine whether any deviations from a normal distribution are statistically significant and, if necessary, to revise the distribution.

This work was based on only a single structural geometry and a single set of load conditions, whereas the design procedures must be conservative for a very wide range of both. Although the basic problem described in Chapter 2 was chosen because of practical design interest, there can be no assurance that the conditions represent the most stringent possible, so other conditions could also be of interest. Altering the load conditions would not have much effect on the difficulty of the present analyses, but a change to a full two-dimensional geometry would increase the computational requirements by one or two orders of magnitude.

The extrapolation to end of life was applied in this work to both the design analysis and the sensitivity study. Evaluating the conservatism of this procedure might be possible by comparing the results of the extrapolation of a ten-cycle analysis with an analysis that is carried all the way to failure. Experimental evaluation of this procedure also seems desirable, however.

It would be helpful in evaluations of conservatism if the strain limits of CCN47 could be reconsidered to make a clear distinction between the minimum requirements for an acceptable design and additional margins that are incorporated for safety.

Finally, structural testing to failure is the most urgent need of all. As discussed in Chapter 7 and illustrated in Fig. 7.1, there are many sources of uncertainty in inferring structural behavior from a design analysis, and heat-to-heat variability is only one of those. Most others can only be assessed by actual testing to structural failure.

9. SUMMARY AND CONCLUSIONS

A sensitivity study was carried out to determine the effect of heat-to-heat variability of type 304 stainless steel on the results of a pipe ratchetting analysis. A design analysis using property data from the NSMH and incorporating the usual sources of conservatism was also performed. The conservatism of the design analysis was assessed by comparing it with the sensitivity study.

For ratchetting strain, when no allowances were made for conservatism built into the inelastic ratchetting strain limits [1% on mean strain, 2% on linear strain, and 5% on peak strain, as specified by CCN47 (Ref. 6)], heat-to-heat variability was found to cause nonconservatism of the recommended design analyses in a majority (51 to 89%) of the heats. (Because the safety factors incorporated into the strain limits are unknown, allowances could not be made for them.)

In the case of creep damage and the cyclic life based on unit creep damage, the design margins of CCN47 are known. In about 1% of the heats, the design margins were found to be insufficient to compensate for heat-to-heat variability.

In the case of fatigue damage and the lifetime based on extrapolation to unit fatigue damage, none of the one million randomly selected heats were found in which the heat-to-heat variability caused the code design margins to be exceeded.

Because some nonconservatism was calculated for the present design procedure, the effect of introducing an added design margin was considered in the form of a simple factor that was multiplied by the ratchetting strains or damages or divided into the lifetimes calculated by the design analysis to obtain a revised design analysis result. An added safety factor of about 1.7 to 2.2 was found to reduce the percentage of nonconservatism by an order of magnitude. Although a still lower percentage of nonconservatism might be desirable in design, a calculation of a very low percentage of nonconservatism based on the present work might require an unacceptable degree of extrapolation of the sensitivity study results. If a small allowable percentage of nonconservatism were definitely established, a sensitivity study could possibly be tailored to establish the added safety factor required with a minimum of extrapolation. Such a modified sensitivity study could easily involve an order of magnitude more computation, however.

To arrive at a definite required safety factor from the results of this work, an allowable percentage of nonconservatism must first be prescribed. The authors believe that some investigations of the consequences of nonconservatism would be required to provide a basis for the specification of an allowable percentage of nonconservatism.

ACKNOWLEDGMENTS

The authors wish to thank J. M. Corum, who suggested this study, and J. A. Clinard and R. L. Huddleston, who reviewed the manuscript.

REFERENCES

1. T. W. Pickel et al., "Study of Thermal Ratchetting Behavior and Elastic Design Requirements," *High-Temperature Structural Design Methods for LMFBR Components Quart. Prog. Rep. Sept. 30, 1972,* ORNL/TM-4058, pp. 190–213.
2. J. M. Corum and W. K. Sartory, *Analytical Study of Elastic Creep-Fatigue Design Rules for ASME High-Temperature Code Case,* ORNL/TM-4710 (August 1975).
3. W. K. Sartory, *Analytical Investigation of the Applicability of Simplified Ratchetting and Creep-Fatigue Rules to LMFBR Component Geometries—Two-Dimensional Axisymmetric Structures,* ORNL/TM-5616 (December 1976).
4. G. T. Yahr, *Simplified Analysis Methods for High-Temperature Structural Design. Summary of Phase I Study,* ORNL-5289 (October 1977).
5. U.S. Department of Energy, *Nuclear System Materials Handbook,* Vol. 1, Book 1, Sect. 2, "304SS Annealed," Hanford Engineering Development Laboratory, Richland, Wash.
6. ASME Code Case N-47-13, *Cases of ASME Boiler and Pressure Vessel Code,* American Society of Mechanical Engineers, New York, 1978.
7. J. M. Corum and W. K. Sartory, "Comparison of Inelastic Analysis Predictions with Test Results for Test Series 1 and 2," *High-Temperature Structural Design Program Prog. Rep. Period Ending Dec. 31, 1974,* ORNL-5048, pp. 202–206.
8. C. C. Shultz, "Consistent Creep and Rupture Properties for Creep-Fatigue Evaluation," Paper No. 79-PVP-30, Pressure Vessel and Piping Conference, San Francisco, June 25–29, 1979.
9. W. J. McAfee and W. K. Sartory, *Materials Heat-to-Heat Variability Study: Part I—Compilation and Analysis of Data,* ORNL-5604 (to be published).
10. Letter from J. M. Corum, ORNL, to Members, RDT Standard F9-4 Task Force, Oct. 4, 1978; Subject: Proposed Modifications to RDT Standard F9-5T Inelastic Analysis Guidelines.
11. U.S. Energy Research and Development Administration, *Guidelines and Procedures for Design of Nuclear Systems Components at Elevated Temperatures,* RDT Standard F9-5T (September 1974).
12. D. R. Diercks and D. T. Raske, *Elevated-Temperature Strain-Controlled Fatigue Data on Type 304 Stainless Steel: A Compilation, Multiple Linear Regression Model and Statistical Analysis,* ANL-76-95 (December 1976).
13. W. K. Sartory, *PLACRE User's Manual,* ORNL/TM-5626 (February 1977).
14. G. A. Greenbaum and M. F. Rubinstein, "Creep Analysis of Axisymmetric Bodies Using Finite Elements," *Nucl. Eng. Des.* **7,** 379 (1968).
15. P. V. Marcal and I. P. King, "Elastic-Plastic Analysis of Two-Dimensional Stress Systems by the Finite Element Method," *Int. J. Mech. Sci.* **9,** 143 (1967).
16. J. Crank and P. Nicholson, "A Practical Method for Numerical Evaluation of Solutions of Partial Differential Equations of the Heat-Conduction Type," *Proc. Cambridge Philos. Soc.* **43,** 50 (1947).
17. C. Lanczos, *Applied Analysis,* p. 245, Prentice-Hall Englewood Cliffs, N.J., 1956.

ORNL-5605
Dist. Category UC-79,
-79h, -79k

Internal Distribution

1. R. L. Battiste
2. J. J. Blass
3. S. E. Bolt
4. C. R. Brinkman
5. J. W. Bryson
6. J. P. Callahan
7. S. J. Chang
8. J. A. Clinard
9. C. W. Collins
10. W. E. Cooper
11–19. J. M. Corum
20. W. G. Dodge
21. J. R. Ellis
22. W. L. Greenstreet
23. A. G. Grindell
24. R. C. Gwaltney
25. W. O. Harms
26. R. F. Hibbs
27. R. L. Huddleston
28. S. K. Iskander
29. P. R. Kasten
30. R. T. King
31. R. L. Klueh
32. R. E. MacPherson
33–41. W. J. McAfee
42. H. E. McCoy
43. H. C. McCurdy
44. J. G. Merkle
45. S. E. Moore
46. E. T. Onat (consultant)
47. P. Patriarca
48. H. Postma
49. C. E. Pugh
50. J. L. Rich
51. M. Richardson
52. D. N. Robinson
53. G. C. Robinson
54–62. W. K. Sartory
63. V. K. Sikka
64. G. M. Slaughter
65. J. E. Smith
66. J. P. Strizak
67. R. W. Swindeman
68. H. E. Trammell
69. D. B. Trauger
70. G. D. Whitman
71. G. T. Yahr
72. Patent Office
73–74. Central Research Library
75. Y-12 Document Reference Section
76–81. Laboratory Records Department
82. Laboratory Records (RC)

Subcontractors

83. H. Armen, Jr., Grumman Aerospace Corp., Bethpage, NY 11714
84. C. E. Jaske, Battelle-Columbus Laboratories, Columbus, OH 43201
85. W. J. O'Donnell, O'Donnell and Associates, Pittsburgh, PA 15232
86. D. H. Pai, Foster-Wheeler Energy Corp., Livingston, NJ 07029
87. C. C. Schultz, Babcock and Wilcox Co., P.O. Box 835, Alliance, OH 44601

External Distribution

88–89. Director, Division of Reactor Research and Technology, Department of Energy, Washington DC 20545
90. Assistant Manager, Energy Research and Development, DOE, ORO
91. Director, Nuclear Research and Development Division, DOE, ORO
92–299. Given distribution as shown in DOE/TIC-4500 under categories UC-79, -79h, -79k